Preprints are preliminary reports that have not undergone peer review.
They should not be considered conclusive, used to inform clinical practice,
or referenced by the media as validated information.

Discovery of Deccan Inclination Anomaly and its possible geodynamic implications over the Indian Plate

S J Sangode (sangode@unipune.ac.in)
Savitribai Phule Pune University
Ashish Dongre
Savitribai Phule Pune University
Amarjeet Bhagat
Savitribai Phule Pune University
Dhananjay Meshram
Savitribai Phule Pune University

Research Article

Keywords: Deccan traps, Palaeomagnetism, Indian plate, Reunion hotspot, Late Cretaceous

Posted Date: September 27th, 2021

DOI: https://doi.org/10.21203/rs.3.rs-900612/v1

License: This work is licensed under a Creative Commons Attribution 4.0 International License.
Read Full License

Abstract

The rapid northward drift of the Indian plate during Deccan volcanism assumes a gradual shallowing of paleomagnetic inclinations in subsequent lava flow formations. A comparison of palaeomagnetic data produced during the last six decades reveals an inclination anomaly during Chron C29r (66.398–65.688 Ma) along with brief clockwise-counter-clockwise rotations during and after the main phase Deccan eruption. This interval temporally coincides with *i)* an accelerated Indian ocean spreading rates, *ii)* brief incursion of an inland 'seaway' and *iii)* a major drop in the sea level at the southern tip of the Indian Peninsula. Furthermore, the restoration of tilt later during C29n agrees with the withdrawal of the inland seaway and the development of a regional southward dip of the Deccan lava flow formations. Here, we produce an evolutionary model to postulate the interaction of the Réunion plume with the Indian lithospheric plate with coincident geological evidences demanding further exploration.

Introduction

Recent studies on mantle plume-lithosphere interactions indicated that spreading plume heads below the lithosphere can develop significant asthenospheric flows to exert the 'plume-push' force and act as potential drivers for accelerated plate motions and/or initiation of subductions (e.g., Pusok and Stegman 2020; Cande and Stegman 2011; van Hinsbergen et al. 2011). The Deccan large igneous province (LIP) is the product of lithospheric interactions of the Réunion hotspot over the northward drifting Indian plate during Late Cretaceous and early Paleogene times (Courtillot et al., 1986; Basu et al., 1993). Geochronological records indicate a tholeiitic basalt peak during 66.4–65.4 Ma, i.e., precisely within the geomagnetic Chron C29r. This peak is widely referred to as the Main Deccan eruption phase (Sprain et al., 2019 and references therein), denoted here by the DE_M. However, the style and repercussions of the impact of the Réunion mantle plume over the Indian lithospheric plate are inadequately explored (e.g. Raval and Veeraswamy 2019).

Globally, Deccan traps represent one of the classical palaeomagnetic records with extensive databases that were produced during the last six decades (e.g., Clegg *et al.*, 1955, Vandamme et al., 1991; Wensink 1973; Chenet et al., 2008; 2009). We considered over 1600 statistically significant mean directions obtained from all over the Deccan trap flows and dikes (Fig. 1).

The high ferrimagnetic concentrations in the Deccan basalt mineralogy enabled classical approaches of successful demagnetization to obtain the characteristic remanence (ChRM) directions referred to as primary magnetization. Here, we compiled the data from 56 widely referred publications representing the entire Deccan province, although they were largely dominated by Central Province and Chron 29r. After compilation, we classified the data into geomagnetic Chrons C30n, C29r and C29n (methods and treatment of data described below and the compiled data are available in Supplemental file). As mentioned, the Chron 29r (66.398 Ma – 65.688 Ma) represents the highest number of data points in agreement with the prevailing knowledge that over 80% of the lavas erupted during this D_{EM} Chron (e.g. Renne et al., 2015; Schoene et al., 2015; Sprain et al., 2019). The compilation observed an unambiguous inclination anomaly of more than 10º and clockwise + anticlockwise rotations of 2 to 5 degrees during C29r (see Tables 1 and 2 and the data treatment in sections below).

Table 1
An account of the mean paleomagnetic data recalculated from the database (presented in Supplemental file).

	Total data points	Mean D/I	Super-pole	Mean Inclination Data		
				C30n	C29r	C29n
Vandamme et al. (1991)	163	154/43 (antipode: 334/-43)	281˚E 37˚N	D/I —	D/I 154/44	D/I 333/-48
This Study	1062	152/56 (antipode:332/-56)	284˚E 27˚N	333/-38	157/47	341/-32
Expected Inclinations with Deccan Age-latitude relation (van Hinsbergen et al 2015)				38	35	32
Inclination Anomaly				—	12	—

Methodology

The inferences and conclusions drawn in this manuscript are based on the palaeomagnetic database developed from published literature to date (from 1955 to 2020). Over 65 publications presenting palaeomagnetic approaches were published during this time, out of which over 50 publications were widely and repeatedly referred independently or as cross references. The vast majority of these papers unambiguously reported directions in agreement with the N-R-N sequence of the C30n-29r-29n geomagnetic polarity time scale. These data were produced globally by different teams, and the analysis was performed in many different reputed laboratories with varied sets of instrumental configurations and sensitivities. We elaborate here on the criteria and methods adopted to compile and treat the data. We also describe the sources of error and the rationale of filtering the data for mean calculations.

The published papers generally presented demagnetization data (using thermal or alternating fields) and the estimation of characteristic remanent magnetization (ChRM) as primary remanence. The routine statistical methods of spherical distribution used in paleomagnetism allowed the means to be estimated at the specimen level and then at the sample level and site levels. It enabled standard parameters (e.g., Alpha-95, precision parameter and maximum angular deviations) to describe their scatter, facilitating global comparison. It further gives an idea about the quality of data in addition to describing the normal/reverse polarities and calculating the apparent and true poles. Routine statistical methods are based on the classical approach of Fisher statistics (Fisher, 1967) for spherical distribution of the vector data. This criterion has been used universally for rejection of the data and depiction of its quality.

In the majority of the papers, the reversal is unambiguously assigned to C29r, the reversal followed by normal to C29r-29n, and the normal followed by reversal to 30n-29r polarity chrons. The data are very well supported by field stratigraphic knowledge or chemostratigraphy. For the present analysis, we complied only with the declination/inclination (D/I) directions from the published literature, facilitating the site mean data points (given in the supplementary file). This is because the NRM intensities are found to have large deviations due to style of presentation and laboratory standards and instrumental sensitivities from individual attempts. Palaeomagnetic analysis involves various protocols of demagnetization adopted by different workers and instrumental sensitivities. Therefore, the standardization and comparison of NRM intensities across different attempts is not feasible. However, since our inferences are founded entirely on the D/I data, the NRM intensities are not considered further.

Possible Sources of Error

The data were retrieved and rechecked several times to check the typo errors. Below, we discuss the sources of errors based on which the filtering strategy was adopted.

1) Manual error

The first and foremost source of error is generally developed during the collection of oriented samples in the field. The oriented samples are collected manually (oriented hand samples) or by gasoline-driven portable rock coring machines (manually handled). The samples were marked carefully using either the north compass or the sun compass method. This has a greater chance of introducing manual errors at various stages from marking in the field to creating cylindrical specimens in the laboratory. Manual errors can also be introduced during laboratory handling of specimens. For most spinner magnetometers, the samples are to be handled over six directions of measurements at every stage. There is no clue to define the manual error, although it may be represented in the final data as scatter that can be defined by the standard palaeomagnetic data presentation procedures but with unknown contribution.

2) Laboratory standards: The palaeomagnetic data in Deccan traps are produced from various laboratories that are commonly equipped with spinner magnetometers. The high NRM intensities often permit complete demagnetization, even with routine spinner magnetometers with low sensitivities (e.g., Minispin from Molspin UK, Sensitivity: 0.05 mA/m). The other common spinner magnetometers of better sensitivities used are the DSM-Schonstedt (~ 10e-4 A/m) and the JR-4 to 6 series of AGICO Czech (~ 2.4 x μA/m). Both of these instruments thus provide better confidence over a large number of palaeomagnetic data, although the quality of data carefully produced from other instruments, such as Astatic magnetometers, is ascertained considering the excellent repeatability and the higher intensities of the Deccan basalt samples. Furthermore, the fully automated AGICO instruments prevent manual errors of sample positioning, and the standardized data interface software, statistics and plotting interface allows rapid, error-free processing. The cryogenic magnetometer (e.g., 2G) gives the finest sensitivity in paleomagnetic analysis; however, the strong remanence in Deccan basalt does not demand such analysis unless paleointensity and secular variation such as studies are aimed.

The detailed palaeomagnetic analysis involves demagnetization of a large array of specimens to produce statistically significant data by the removal of noisy results. The two most common methods of demagnetization used are thermal and alternating field demagnetizations. While thermal demagnetization can introduce laboratory-induced errors during heating and cooling, af demagnetization is most successful in Deccan traps due to its soft ferrimagnetic mineralogy for both primary and secondary components. Individual workers have used different protocols of demagnetization strategy, and the demagnetizers themselves can introduce spurious fields during analysis, producing deviations rather than direct errors. Furthermore, the skills and experience of individual workers during interpretation varies, which may lead to some manual bias error component.

a) Geomagnetic variability and transitional fields: Some authors have indicated secular variation or the non-dipole field as the source of error in paleomagnetic directions acquired by few samples. However, such samples are most likely to be rejected, showing spurious directions, as the palaeomagnetic directions for Deccan traps are very well known and constrained. Similar is the case for the transitional polarity instances from normal to reversal and vice versa. These directions are also likely rejected by the individual authors, and if they are present in the data, our filtering criteria have taken care of removing such intermediate directions.

b) Geotectonics: The shield type geometry of the Deccan province in general refutes any major intra-shield tectonics to affect the palaeomagnetic directions. However, the lineaments and other structural features within Deccan Province, if contemporary, can be inferred for tectonically induced errors. Few authors have reported such tectonic relations, but they are mainly related to vertical movement rather than internal rotations and deformation and do not express any major anomaly in paleomagnetic data. These references justifying the tectonic component are avoided in our database approach. Chron C29r is the main focus of this study, and the majority of the palaeomagnetic data for this chron belong to the main/central Deccan province, which does not show such intra-shield tectonics at large to affect the internal rotations and tilt. If such incoherence is present, it should be reflected by deviation of D/I directions internally, for which we have applied the filtering criteria discussed below.

Data Reduction (rejection) and Filtering

The Deccan traps represent one of the richest databases for a short geological interval of less than 5 Ma, marked by the distinct polarity zone of N-R-N of the Late Cretaceous/Paleogene. The ample data produced globally from different laboratories are within close agreement, and a simple filtering and reduction of data based on routine spherical distribution statistics is feasible.

A previous compilation made by Vandamme et al. (1991) resulted in defining the Deccan Super pole based on contemporarily available data. With the updated database up to 2020, we recalculated the Deccan Super pole, which is in close agreement with Vandamme et al 1991 (see Table 1). The deviation of values seen in this table is simply due to enrichment by the new data during the latter 30 years since the publication of Vandamme et al 1991. Therefore, considering these Super pole directions as central tendencies, we defined the limits/windows for filtering out the data, apart from rejecting the data with large scatter defined by the precision parameter (k) and alpha-95 of Fisher statistics.

Table 2
Considering the means for whole data in 5th column of Table 1 as the central tendency of the updated database, we further applied filters to remove the noise in data due to the possible errors described above. The data for C30n, C29r and C29n are filtered individually in a declination window of +/- 36 (10% of 360) and inclination window of +/-18 (10% of 180).

	Chron 30n		**C29r**		**C29n**	
	D	**I**	**D**	**I**	**D**	**I**
Central Tendency	333	-38	157	47	341	-32
Window	297–366	20–56	121–193	29–65	305–377	14–50
Means after Filter	338	-38.7	153.3 (333.3 antipode)	47.4	334.8	-35.1
Stats	A95: 2.5; k = 21.37, N:153		A95: 1.1, k = 36.05, N: 451		A95: 4.3, k:21.61, N:54	
Anomaly with Vandamme et al. 1991	+ 4 (clockwise)	-5 (shallow)	-0.7 (anticlock)	+ 5 (deeper)	+ 0.8 (clockwise)	-8 (shallow)
Anomaly with expected inclination at Réunion latitudes		0.7		12.4		3

Table 3
The Inclination Anomaly for C29r with respect to inclinations from various approaches described in text (inclination for C29r is taken as 47).

Reference	Inclination in degrees	Anomaly Amount in Degree
w.r.t. Expected latitudes by *tan I = 2 tanλ* *(λ = 20.5 to 21.5)*	~ 36 to 38	11 to 9
w.r.t. C30n	38 (Table 1)	9
w.r.t. C29n	32 (Table 1)	15
w.r.t. C30n Filtered Mean	47.4–38.7	8.7
w.r.t. C29n Filtered Mean	47.4–35.1	12.3
w.r.t. latitudinal mean	47.4–37	10.4
Average for expression in the text……..		10.78

Table 4
Rotational anomaly (+: clockwise, -: anticlockwise).

	Filtered Mean	Wrt Reference North	Inferred Indian plate rotation
29n	334.8	-25.2	2 degree anticlockwise wrt 29r
29r	333.3	-26.7	5 degree clockwise wrt 30n
30n	338	-22	
During 80 to 60 Ma		-12	

The Inclination Anomaly and Rotation

The observed mean inclination for C29r is significantly higher than the anticipated paleolatitude derivative of 35º, and an average value of 10.78 can be assigned from various approaches expressed in Table 3. This ‘+10º’ inclination anomaly observed during C29r is simply a mathematical expression of a significant northerly dip of the Indian plate. It is much oversighted in the context of equatorward drift of the Indian plate, which anticipates either inclination shallowing or, at most, inclination values intermediate to C30n and C29n. Moreover, no record of such large magnitude changes during the Late Cretaceous geodynamo does exist (Coe *et al.*, 2000; Pechersky *et al.*, 2010; Velasco-Villareal *et al.*, 2011) and therefore also refutes the geodynamo effect. In contrast, coincident geological evidence from the Indian subcontinent endorses the anomaly by possible effects of plate tilting (Fig. 2 and the evidence produced below).

Very high inclinations (D/I=140/60º) during C29r are reported from the Deccan trap rocks of the Cauvery region in southern India (Mishra *et al.* 1989), and although the data are inadequate, they suggest a southern extent. The pre-Deccan Late Cretaceous strata from the Cauvery Basin on the southern Peninsula record a shallower inclination (338/-38, N=80) (Venkateswarulu 2020), substantiating the existence of the Deccan anomaly. The inclinations for C29n and C30n agree well with the anticipated paleolatitudes (Table 3), which indicates that the tilt was absent in C30n and restored during C29r as the Indian plate drifted away from the Réunion plume head (e.g., see Fig. 2). The regional southward dip for the Deccan lava flows (Fig. 3) is widely documented (Jay and Widdowson 2008; Shoene *et al.* 2015) and verify our proposed model based on palaeomagnetic inclination (Figure 3).

Considering the tilt and rotation estimates from the palaeomagnetic database (Tables 1 to 4), we further confirm our model by supporting geological evidence accounted below.

Magmatic records of plume head arrival and plate tilt

There is a close temporal and spatial linkage between voluminous LIPs, their tholeiitic and alkaline magmatism and mantle plumes (e.g., Bryan and Ernst 2007). The LIPs are generally characterized by short-lived (<1-5 Ma) igneous pulses responsible for large volume (>75%) magma outpours. Alkaline rocks associated with LIPs are typically formed due to low degrees of partial melting of mantle owing to minor thermal effects from an impinging or receding mantle plume (e.g., Gibson *et al.* 2006). The impact of the Réunion plume over the Indian plate is in close agreement with this convention through the observed episodes of tholeiitic and alkaline magmatism. The initial impact of the Réunion plume head started ~0.2 million years before the DE_M and produced nepheline syenites and alkali gabbros during these early Deccan eruptions (Fig. 3), corresponding to terminal C30n/early C29r. Recent high-precision geochronological data (Renne *et al.*, 2015; Sprain *et al.*, 2019) indicated outpouring of bulk Deccan tholeiites between 65.4 and 66.4 Ma within C29r. This rapid extrusion requires higher amounts of partial melting under a considerably elevated geothermal gradient during a fully developed plume head, which precisely coincides with the duration of C29r (Cande and Kent, 1995). Small-volume volatile-rich magmatism of lamprophyres and carbonatites between 65.8-65.2 Ma (Fig. 3), which was mostly emplaced towards the terminal part of the $DE_{M,}$ typically intruded the Deccan lavas. This terminal phase is an artifact of small-fraction melting caused by thermal weakening during the waning stage of the Réunion plume. The occurrence of DE_M precisely within C29r therefore elucidates the short span (<1 million years) of geodynamic interaction of the plume head with the Indian plate. This rapid impact of the plume head below the western margin of the Indian plate therefore appears to have resulted in tilt and rotation, as recorded by the paleomagnetic data.

Accelerated convergence at the end of C29r

The spreading rates in the Indian Ocean reached a maximum between ~66 and 63 Ma during C29n (Cande and Stegman, 2011; compiled and redrawn in Fig. 4). The initial anomalously high rates of drift of the Indian plate from less than 100 mm/y to ~160 mm/y during 68 to ~66 Ma are explained by the arrival of the plume head (Eagles and Hoang, 2014). Therefore, the later increase in spreading (up to 180 mm/y after ~66 Ma) during the waning and withdrawal stages of the plume/plume head needs to be explained.

We postulate this later increase in convergence rates as a result of *i)* the termination of plume-induced rotational and tilt components that resolved into northward drifting kinematics, in addition to *ii) the* establishment of double subduction.

Acceleration of the intra-oceanic subduction

Mantle plumes have been considered drivers of regional subduction initiation (Gerya *et al.* 2015; Pusok and Stegman 2020; van Hinsbergen *et al.* 2021, Rodriguez *et al.* 2021). Multiple subductions are evident for the India-Asia convergence; however, the final subduction during ~66 Ma to 65 Ma is little explored in the context of Deccan volcanism and the Réunion plume push force. We infer that the quick geodynamic response of the Indian plate over the Réunion plume head during DE_M marked by the tilt and counter rotations during C29r might have exerted significant changes in pre-existing plate kinematics at the India-Asia subduction interface. Possible resultant deformation due to plate tilt and rotation added to the previously accelerated rate of convergence may have significant repercussions on the initial stage of intraoceanic subduction (Fig. 2). The combination of quick clockwise and anticlockwise rotations along with tilt and drift appears to have superimposed over the pre-existing kinematics for the Indian plate demanding detailed kinematic modelling in this context.

Opening of the 'Sea-way' within the plate

Based on paleontological finds, a short-lived 'seaway' associated with Deccan traps has been reported precisely at the end of C29r (e.g. Keller *et al.* 2009, 2012). This inland 'sea-way' formation (/marine influence) along pre-existing rift valleys (i.e. Narmada and Godavari Rifts, shown in Fig. 3) is evident by the stressed marine fauna. The brief north/northeast tilting of the Indian plate therefore offers a possibility to explain the formation of the brief inland 'sea-way'.

Biostratigraphically well-documented localities ~800-1000 km inland of the Narmada and Godavari rifts contain brief and stressed planktic foraminiferal assemblages within terrestrial palustrine to freshwater facies (Keller et al 2009, 2012). The absence of benthic species among these localities (Keller et al 2012) indicates only a brief marine incursion that can be explained by a major tectonic event such as the lithospheric tilt reported here. The paleosols developed over this zone designate upland conditions and further support the restoration of tilt during C29n, as depicted in Figure 2. The late Maastrichtian rocks of the Cauvery Basin at the southern tip of Peninsular India represent fluvial formations overlain by marine to estuarine formations and record a vertical sea level fall of 80 m (Nagendra and Reddy 2017; Raju et al 1994). Thus, upliftment of the southern peninsular tip of the Indian plate is documented and marked by a rapid sea level fall during the deposition of the Kallamedu Formation (Late Maastrichtian) in the Cauvery Basin. The contemporaneous upliftment of the southern end of the Indian plate along with downward tilt in northern and northeastern Deccan provinces indicate plume head-induced tilting.

Finally, although more geological evidence with precise dating is required, the present perceptions (Fig. 2-4 and Table 4) strongly support the geodynamic developments over the Indian plate precisely during C29r and the main Deccan eruption.

Table 5: A summary of sequence of events presented in the paper.

Time	Stage	Event
30n	Plume early stage	Indian plate encountered the Réunion hotspot
Late 30n to Early 29r	Emerging plume-lithosphere interaction	Indian plate encountered the plume over western continental margin and rotated clockwise possibly by thermal expansion (and uplift) of the lithosphere in the plume region. Eruption of early lavas and alkaline rocks. Acceleration of spreading rates.
Early to Late 29r	Fully developed plume head	Maximum exposure of the plate to plume, eruption of bulk of Deccan basalts, possible upliftment of the southern Peninsular part of the Indian plate along with tilting in the N/NE part of the plate, biostratigraphic evidences of 80m drop in sea level in south and opening of the seaway in N/NE periphery of Deccan. Quick clockwise-anticlockwise rotations along with northward tilt appears to have developed a weak zone possibly leading to the latest subduction in the India-Eurasia zone.
29n		Waning stage of the plume, restoration of tilt, regional south dip of Deccan, closure of seaway, onset of secondary subduction

The present findings have larger implications for understanding the plate-wide impact of plume-lithospheric interactions. This may further lead to detailed investigations on the response of concurrent geological consequences related to Réunion plume-lithospheric interactions over the Indian plate during Deccan trap volcanism.

Declarations

Acknowledgements

We indirectly acknowledge all the authors who produced and published the palaeomagnetic data over the years cited in this paper. SJS, AND AB acknowledge Ministry of Earth Sciences for the grant MoES/P.O.(Seismo)/1(353)/2018. All the authors acknowledge Head, Department of Geology SPPU, for support during the pandemic.

There are no conflict of interests.

References

Basu, A.R., Renne, P.R., Dasgupta, D.K., Teichmann, F., Poreda, R.J., 1993, Early and Late Alkali Igneous Pulses and a High-3He Plume Origin for the Deccan Flood Basalts. Science 261, p. 902–906.

Bryan, S. and Ernst, R., 2008, Revised Definition of Large Igneous Province (LIP), Earth Science Reviews. doi: 10.1016/j.earscirev.2007.08.00.

Cande, S.C. and Kent, D.V., 1995, Revised calibration of the geomagnetic polarity timescale for the Late Cretaceous and Cenozoic. Journal of Geophysical Research, 100, p. 6093–6095.

Cande, S.C. and Stegman, D.R. 2011, Indian and African plate motions driven by the push force of the Réunion plume head. Nature 475, p. 47–52.

Chenet, A.L., Courtillot, V., Fluteau, F., Gérard, M., Quidelleur, X., Khadri, S.F.R., Subbarao, K.V., Thordarson, T., 2009, Determination of rapid Deccan eruptions across the Cretaceous–Tertiary boundary using paleomagnetic secular variation: 2. Constraints from analysis of eight new sections and synthesis for a 3500-m-thick composite section: Journal of Geophysical Research 114/38. doi: 10.1029/2008JB005644.

Chenet, A.L., Fluteau, F., Courtillot, V., Gerard, M., Subbarao, K.V., 2008, Determination of rapid eruption across the Cretaceous–Tertiary boundary using paleomagnetic secular variation: Results from a 1200 m thick section in the Mahabaleshwar escarpment. Journal of Geophysical Research 113 (B4), B04101.

Clegg, J.A., Deutsch, E.R., Griffiths, D.H., 1956, Rock magnetism in India, Philos. Mag., 1, p. 419–431.

Coe, R.S., Hongre, L., Glatzmaier, G., 2000, An examination of simulated geomagnetic reversals from a palaeomagnetic perspective Phil. Trans. R. Soc. A., 358, p. 1141–1170 http://doi.org/10.1098/rsta.2000.0578(2000)

Courtillot, V., Besse, J., Vandamme, D., Montigny, R., Jaeger, Cappetta, H., 1986, Deccan flood basalts at the Cretaceous/Tertiary boundary? Earth and Planetary Science Letters 80, P. 361–374.

Dongre, A., Dhote, P.S., Zamarkar, P., Sangode, S.J., Belyanin, G., Meshram, D.C., Patil, S.K., Karmakar, A., Jain, L., 2021, Short-lived alkaline magmatism related to Réunion plume in the Deccan large igneous province: inferences from petrology, 40Ar/39Ar geochronology and paleomagnetism of lamprophyre from the Sarnu-Dandali alkaline igneous complex. Geological Society London Special Publications 513. https://doi.org/10.1144/SP513-2021-34

Eagles, G. and Hoang, H., 2014. Cretaceous to present kinematics on the Indian, African and Seychelles plates. Geophysical Journal International 196, p. 1–14.

Gerya, T.V., Stern, R.J., Baes, M., Sobolev, S.V., Whattam, S.A., 2015, Plate tectonics on the Earth triggered by plume-induced subduction initiation. Nature, 527, p. 221–225, doi:10.1038/nature15752.

Gibson, S.A., Thompson, R.N., Day, J.A. 2006, Timescales and mechanisms of plume- lithosphere interactions: 40Ar/39Ar geochronology and geochemistry of alkaline igneous rocks from the Parana-Etendeka large igneous province. Earth and Planetary Science Letters 251, p., 1–17.

Jay, A.E. and Widdowson, M., 2008, Stratigraphy, structure and volcanology of the south-easts Deccan continental flood basalt province: implications for eruptive extent and volumes. Journal of the Geological Society London 165, p. 177–188.

Keller, G., Adatte, T., Bajpai, S., Mohabey, D.M., Widdowson, M., Khosla, A., Sharma, R., Khosla, S.C., Gertsch, B., Fleitmann, D., Sahni, A., 2009, K-T transition in Deccan Traps and intertrappean beds in central India mark major marine seaway across India. Earth and Planetary Science Letters 282, p. 10–23. doi:10.1016/j.epsl.2009.02.016.

Keller, G., Adatte, T., Bhowmick, P.K., Upadhyay, H., Dave, A., Reddy, A.N., Jaiprakash, B.C. 2012, Nature and timing of extinctions in Cretaceous-Tertiary planktic foraminifera preserved in Deccan intertrappean sediments of the Krishna-Godavari Basin, India. Earth and Planetary Science Letters 341–344, p. 211–221. doi:10.1016/j.epsl.2012.06.021.

Mishra, D.C., Gupta, S.B., Venkatarayudu, M., 1989, Godavari rift and its extension towards the east coast of India. Earth and Planetary Science Letters, 94, p. 344–352.

Nagendra, R. and Reddy, A.N., 2017, Major geologic events of the Cauvery Basin, India and their correlation with global signatures: A review. Journal of Palaeogeography, 6(1), p. 69–83.

Pechersky, D.M., Lyubushin, A.A., Sharonova, Z.V., 2010, On the synchronism in the events within the core and on the surface of the earth: The changes in the organic world and in the polarity of the geomagnetic field in the phanerozoic. Physics of the Solid Earth 46, p. 613–623.

Pusok, A.E., and Stegman, D.R., 2020, The convergence history of India-Eurasia records multiple subduction dynamics processes. Science Advances 6, eaaz8681.

Raju, D.S.N, Jaiprakash, B.C., Ravindran, C.N., Kalyanasunder, R., Ramesh, P. 1994, The magnitude of hiatus and sea level changes across the K T boundary in Cauvery and Krishna Godavari Basin. Jour. Geol. Soc. India, 44, p. 301–315.

Raval, U., and Veeraswamy, K., 2019, Some apparent space-time mismatches (puzzles) over the Indian subcontinent and channeling. Journal of the geological society of India. 93, p. 25–32.

Renne, P.R., Sprain, C.J., Richards, M.A., Self, S., Vanderkluysen, L., Pande, K., 2015, State shift in deccan volcanism at the cretaceous-Paleogene boundary, possibly induced by impact. Science 350(6256), p. 76–78.

Rodriguez, M., Arnould, M., Coltice, N., Soret, M., Hoang, E., 2021, Long-term evolution of a plume-1 induced subduction in the Neotethys realm. Earth and Planetary Science Letters 561, 116798. https://doi.org/10.1016/j.epsl.2021.116798

Schoene, B., Eddy, M.P., Keller, C.B. and Samperton, K.M., 2021, An evaluation of Deccan Traps eruption rates using geochronologic data. Geochronology, 3, p. 181–198

Schoene, B., Samperton, K.M, Eddy, M.P., Keller, G., Adatte, T., Bowring, S., Khadri, S.F.R., Gertsch, B., 2015, U-Pb geochronology of the Deccan traps and relation to the end cretaceous mass extinction. Science 347, p. 182–184.

Sprain, J., Renne, P.R., Vanderkluysen, L., Pande, K., Self, S., Mittal, T. 2019, The eruptive tempo of Deccan volcanism in relation to the Cretaceous- Paleogene boundary. Science 363, p., 866–870.

van Hinsbergen, D. J. J., Lennart V. de Groot, Sebastiaan J. van Schaik, Wim Spakman, Peter K. Bijl, Appy Sluijs, Cor G. Langereis, and Henk Brinkhuis, 2015, A Paleolatitude Calculator for Paleoclimate Studies (model version 2.1), PLOS ONE

van Hinsbergen, D.J.J., Steinberger, B., Doubrovine, P.V., Gassmöller, R., 2011, Acceleration and deceleration of India-Asia convergence since the Cretaceous: Roles of mantle plumes and continental collision. Journal of Geophysical Research 116. doi:10.1029/2010jb008051.

Vandamme, D., Courtillot, V., Besse, J., Montigny, R. 1991, Palaeomagnetism and age determinations of the Deccan Traps (India); results of a Nagpur– Bombay traverse and review of earlier work. Reviews of Geophysics 29, p. 159–190.

Velasco-Villareal, M., Urrutia-Fucugauchi, J., Rebolledo-Vieyra, M., Perez-Cruz, L., 2011, Paleomagnetism of impact breccias from the Chicxulub crater - Implications for ejecta emplacement and hydrothermal processes. Physics of the Earth and Planetary Interiors 186, p. 154–171.

Venkateshwarlu, M., 2020, New paleomagnetic pole and magnetostratigraphy of the Cauvery Basin sediments, southern India. J Earth Syst Sci 129, 222. https://doi.org/10.1007/s 12040-020-01476-z.

Wensink, H., 1973, Newer paleomagnetic results of the Deccan traps, India. Tectonophysics 17, p. 41–59.

Supplementary File

A supplementary file is not available with this version of the manuscript.

Figures

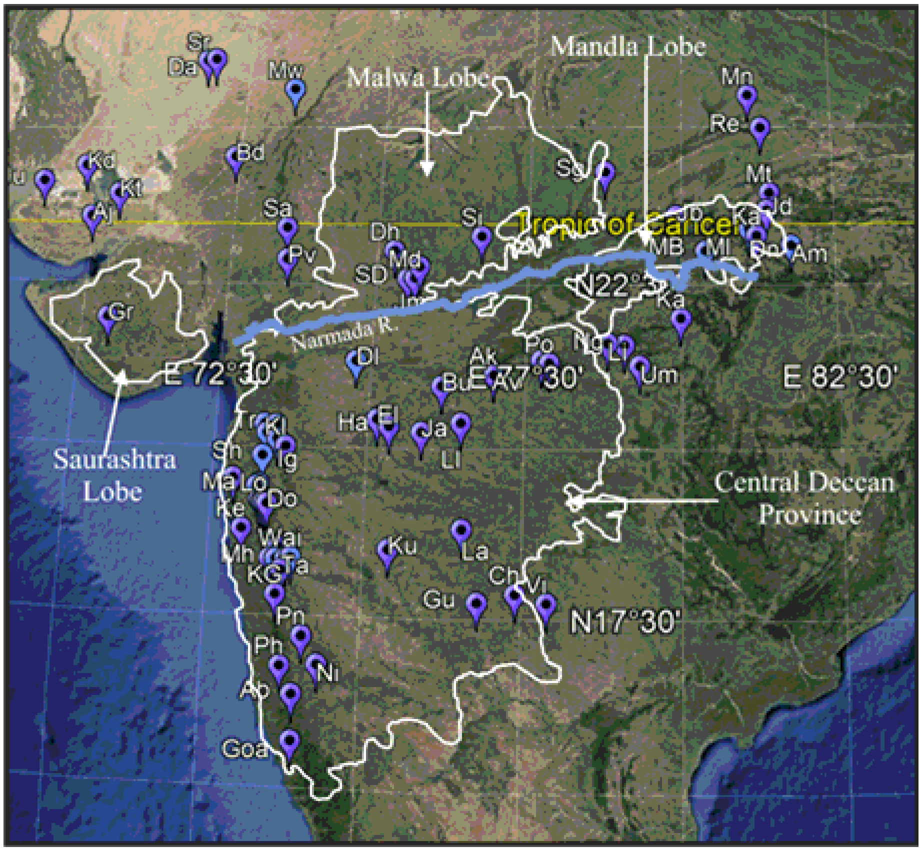

Figure 1

Google image overlay showing the present-day extent of Deccan traps in four distinct lobes (Malwa, Mandla, Saurashtra and Central Province). The lobes (sub-provinces) lying north of the Narmada/Tapi rifts (i.e., Malwa, Mandla and Saurashtra) exhibit the records of the earliest eruptions belonging to Chron C30n as a result of northward drift of the Indian plate after its breakup from Gondwana. The pinned marks with abbreviations (expanded below) are the sites where paleomagnetic studies were undertaken. In the northern region of the central province, the majority of the normal polarity flows overlay the reverse polarity, and the rest of the occurrences with prominent reverse polarity of C29r compile the tripartite subdivision of the Deccan traps into the C30n-C29r-C29n sequence. Stratigraphically thicker (/longer) records of C29r are most widely documented in the Central province. Site Abbreviations- Amboli (Ab) , Anjar (Aj), Akola (Ak), Ambenali (Al), Amarkantak (Am), Amravati (Av), Badargarh (Bd), Buldhana (Bu), Chincholi (Ch), Dandali (Da), Dhar (Dh), Dhule (Dl), Dindori (Dn), Dongargarh (Do), Ellora (El), Goa (Goa), Girnar (Gr), Gulbarga (Gu), Harsul (Ha), Igatpuri (Ig), Jalna (Ja), Jabalpur (Jb), Jodhpur (Jd), Jamdarwaza (Jm), Jumara (Ju), Karopani (Ka), Khairi (Ka), Kalodungar (Kd), Kelgar (Ke), Khumbharli Ghat (KG), Khandala (Kh), Kalsubai (Kl) , Khodala (Ko), Khopoli (Kp), Kanthkote (Kt), Kurduwadi (Ku), Latur (La), Linga (Li), Lonar lake (Ll), Lonavala (Lo), Matheran (Ma), Mandla Bridge (MB), Mandaleshwar (Md), Mahabaleshwar (Mh), Mandla (Ml), Manikpur (Mn), Mokhada (Mo), Mohtara (Mt), Mumbai (Mu), Mundwara (Mw), Neral (Ne), Nagpur (Ng), Nipani (Ni), Panchigani (Pa), Phonda (Ph), Panhala (Pn), Pohor (Po), Pavagadh (Pv), Rewa (Re), Rajahmundry (Rj)Sadara (Sa), Sahastra Dhara (SD), Sagar (Sg), Shahapur (Sh), Singarchori(Si), Sarnu (Sr), Tapola (Ta), Trimbak (Tr), Umred (Um), Varandha Ghat (VG), Vikarabad (Vi), Wai (Wai).

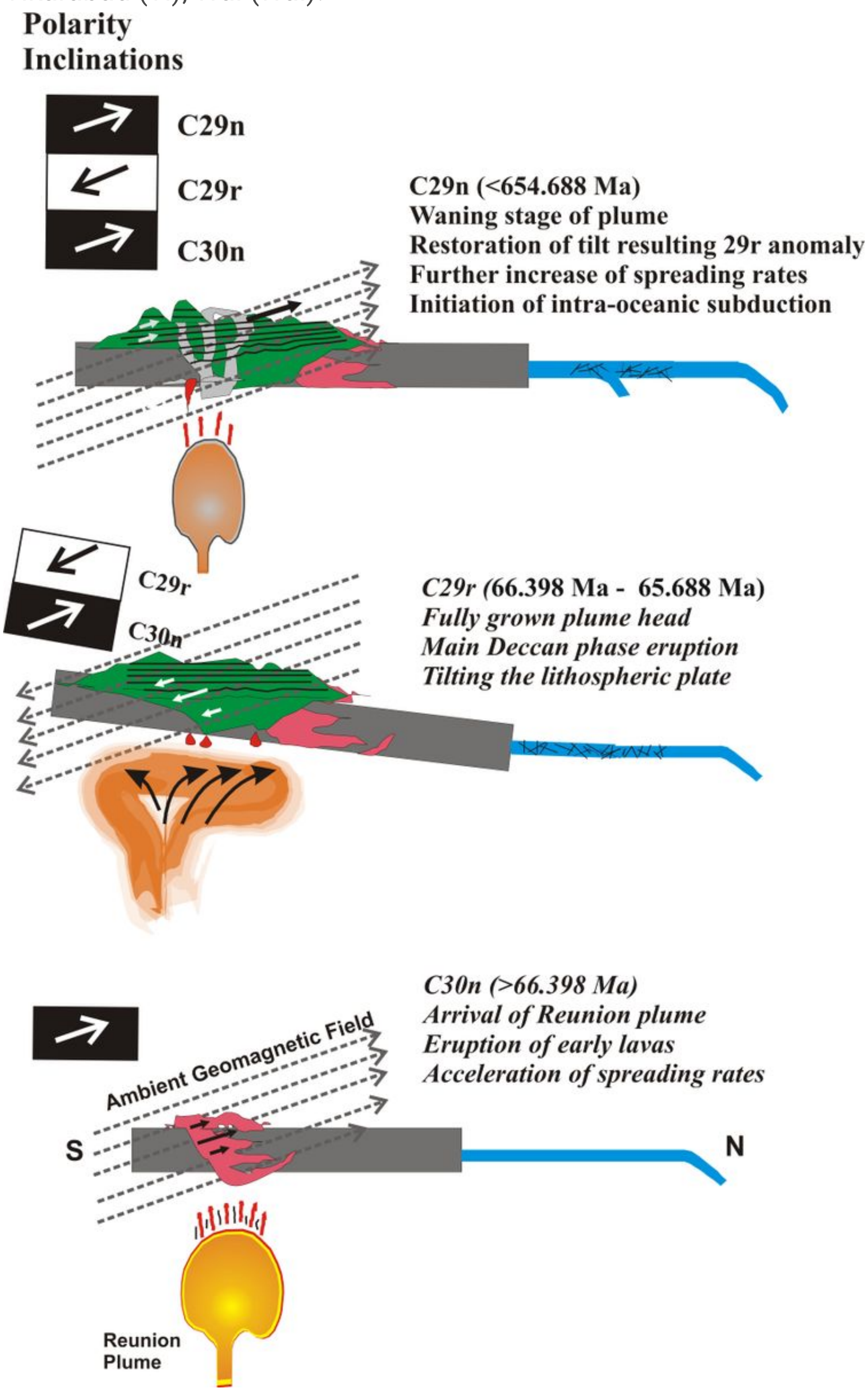

Figure 2

Evolutionary staged model to depict the mechanism of geodynamic interaction of Indian plate with the Réunion plume/hotspot imparting the inclination anomaly. During C30n, the subcontinent approached the impinging mantle plume, as documented by the alkaline magmatism in the northern part of the

Deccan province. The interaction of the Indian plate with a fully developed plume head further during C29r resulted in a north/northeast tilt to record the ambient reverse field. As the plate moved farther from the waning plume, the tilt was restored, and the reverse inclination steepened, producing the inclination anomaly of C29r (detailed in text).

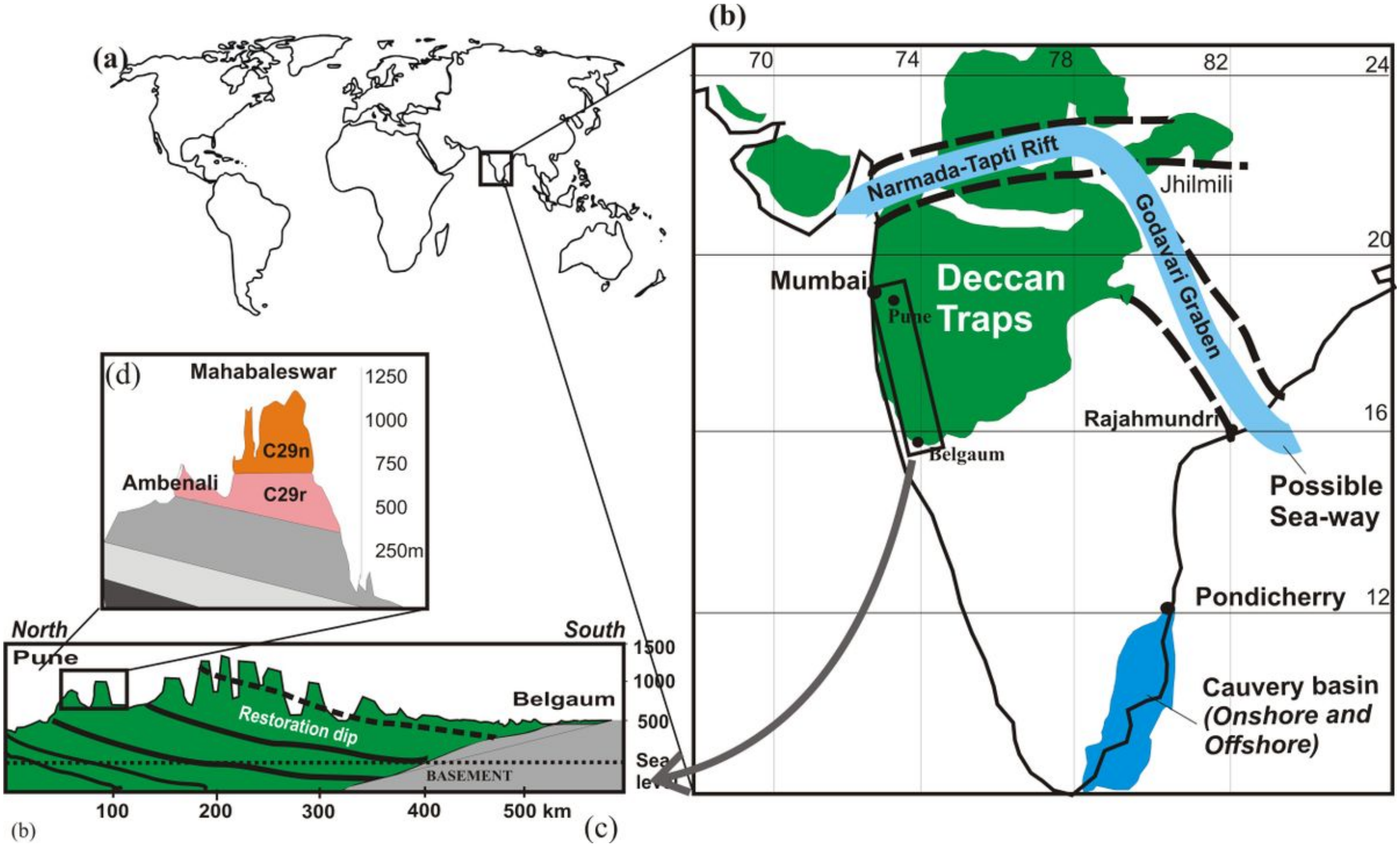

Figure 3

(a) World map showing the location of Deccan Province, (b) India showing the present extent of Deccan trap province and the possible seaway as reported from biostratigraphic records and the location of Cauvery Basin documenting a significant drop in sea level during the Late Cretaceous. The widely reported Pune to Belgaum (N-S) profile (c) depicts a regional dip, explained here as a result of tilt restoration (discussed in text). Inset (d) shows the dip discordance between C29r (Ambenali Formation) and C29n (Mahabaleswar Formation) marked in Schoene et al. (2021), supporting tilt and restoration.

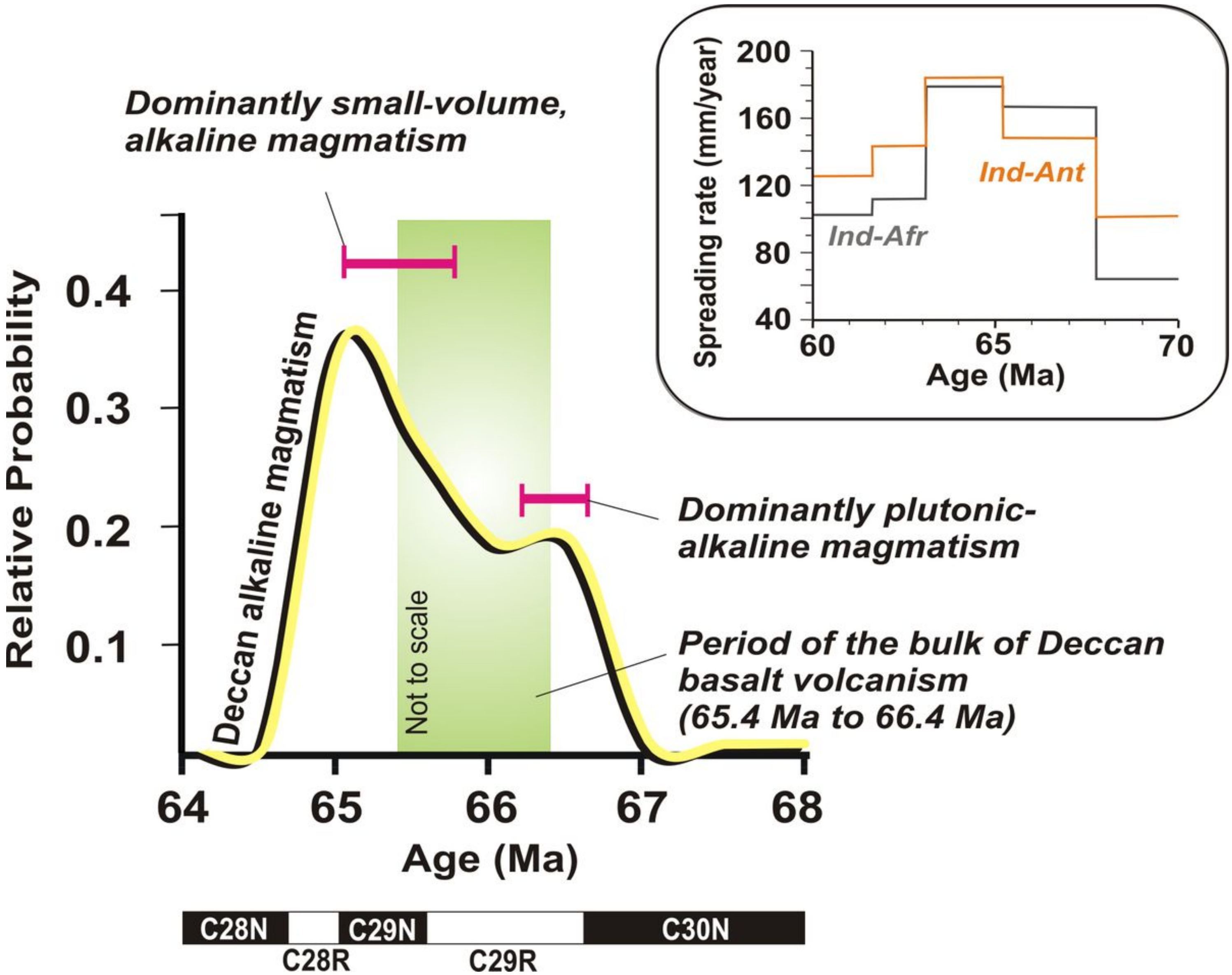

Figure 4

Relative probability of alkaline and small-volume, volatile rich magmatism spatially and temporally related to the Deccan LIP based on high-precision 40Ar/39Ar and U-Pb determinations (n=12) (adopted from Dongre, et al. 2021). The period of bulk Deccan basalt volcanism is also shown in green (from Sprain et al., 2019). Inset: Spreading rates between India-Antarctica and India-Africa ridges (After Cande and Stegman, 2011).